Jason McCormick
e-mail: jason.mccormick@ce.gatech.edu

Reginald DesRoches[1]
e-mail: reginald.desroches@ce.gatech.edu

School of Civil and Environmental Engineering,
Georgia Institute of Technology,
790 Atlantic Drive,
Atlanta, GA, 30332-0355

Davide Fugazza
e-mail: davide.fugazza@samcef.com

Ferdinando Auricchio
e-mail: auricchio@unipv.it

European School for Advanced Studies in
Reduction of Seismic Risk (ROSE School),
and Dipartimento di Meccanica Strutturale,
Universita degli Studi di Pavia,
Pavia, Italy

Seismic Vibration Control Using Superelastic Shape Memory Alloys

Superelastic NiTi shape memory alloy (SMA) wires and bars are studied to determine their damping and recentering capability for applications in the structural control of buildings subjected to earthquake loadings. These studies improve the knowledge base in regard to the use of SMAs in seismic design and retrofit of structures. The results show that the damping properties of austenitic SMAs are generally low. However, the residual strain obtained after loading to 6% strain is typically <0.75%. In general, it is shown that large diameters bars perform as well as wire specimens used in non-civil-engineering applications. The results of a small-scale shake table test are then presented as a proof of concept study of a SMA cross-bracing system. These results are verified through analytical nonlinear time history analysis. Finally, a three-story steel frame implementing either a traditional steel buckling-allowed bracing system or a SMA bracing system is analyzed analytically to determine if there is an advantage to using a SMA bracing system. The results show that the SMA braces improve the response of the braced frames. [DOI: 10.1115/1.2203109]

Keywords: shape memory alloys, damping, recentering, earthquake engineering, innovative systems

Introduction

Over the past few decades, increased population has led to a higher concentration of building structures in moderate to high seismic zones. Recent earthquakes, such as the Northridge earthquake in California (1994), have exposed the vulnerability of these building structures to moderate and strong ground motions. Although these urban events have led to only minimal loss of life, economic losses have been unacceptably high and reached in excess of $50 (US) billion as a result of the Northridge event [1]. Much of this loss can be associated with damage to building structures as a result of large interstory drifts, resulting in catastrophic damage and rendering the structure unable to be occupied and requiring extensive repairs. Past research has shown that concentric bracing systems, passive energy dissipation devices, and recentering devices are effective in limiting interstory drifts. However, these devices have some deficiencies associated with them, such as permanent deformation, requiring parts of the structure or device to be replaced after a seismic event. The search for new technology has led to the consideration of shape memory alloys (SMAs) for vibration control of structures in order to limit interstory and residual drifts by providing added energy dissipation capacity and recentering capabilities to the system.

Shape memory alloys are a unique class of metallic alloys that can undergo large deformations while returning to their original undeformed shape. The ability of shape memory alloys to recover their shape is, in part, due to the ordered crystalline structure between the austenite and martensite phases, which allows the material to undergo a displacive (diffusionless) martensitic phase transformation as a result of a temperature change or an applied stress. On a macroscopic level, the shape recovery occurs through one of two processes, either the shape memory effect, which requires heating of the material above the austenite transformation temperature, or the superelastic effect, which requires only the removal of the applied load or stress. Austenitic or superelastic shape memory alloys recover their shape through the superelastic effect and provide both energy dissipation through a flag-shaped hysteretic behavior and recentering capability through the ability to recover their undeformed shape. Several characteristics of superelastic shape memory alloys make them ideal candidates for seismic applications, such as the ability to provide hysteretic damping, a recentering capability through shape recovery, excellent low- and high-fatigue properties, strain hardening at large strain levels, and the formation of stress plateaus, which limits the force transfer to other members of a structure.

Recently, researchers have conducted several studies to determine the viability of using superelastic shape memory alloys for seismic applications. Several studies have focused on the effect of strain amplitude, loading frequency, cycling, and temperature effects on the mechanical behavior of SMAs [2–5]. Others have looked at the effectiveness of SMAs in actual seismic applications in both bridges and buildings. Dolce et al. [6] found that superelastic SMAs can provide a strong recentering capability when applied to a two-story single-bay reinforced concrete frame as a bracing system. Further results from the experimental testing of large-scale reinforced concrete frames implementing SMA-based devices can be found in Cardone et al. [7] and Dolce et al. [8]. Analytical studies by Baratta and Corbi [9] showed that superelastic braces improved the dynamic response of an elastic-perfectly plastic frame as compared to typical slender elastic-plastic tendons. The use of superelastic SMAs produced a smaller maximum amplitude of response and decreased the residual drifts as a result of the energy dissipation capacity and recentering capabilities of the SMAs. Others have experimentally and analytically shown the benefits of SMA dampers used in building frames [10,11]. Earlier studies by Inaudi and Kelly [12] found that SMA wires can be used in a tuned mass damper system to significantly improve the dynamic response of the structure, particularly when the SMAs are prestressed to the first natural frequency of the structure. The results of these projects show promise for the use of SMAs in seismic applications; however, very few studies have focused on the behavior of large diameter specimens under loading rates and strain levels that are typically experienced during an earthquake.

[1]Corresponding author.

Contributed by the Materials Division of ASME for publication in the JOURNAL OF ENGINEERING MATERIALS AND TECHNOLOGY. Manuscript received August 31, 2005; final manuscript received April 3, 2006. Review conducted by Mohammed Cherkaoui.

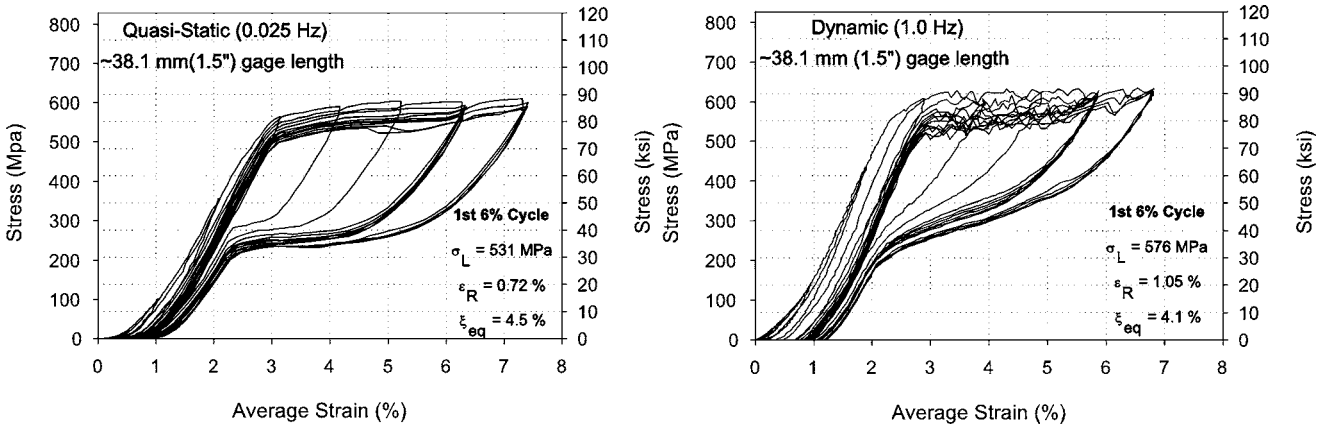

Fig. 1 Stress-strain curves for 0.254 mm (0.01 in.) diameter NiTi shape memory alloys tested at (*a*) 0.025 Hz and (*b*) 1.0 Hz loading rates

Typical past studies have focused on wires and thin bars, where larger diameter sections may be more feasible and economical for earthquake engineering applications in structures.

In order to improve the knowledge base in terms of the use of SMAs in seismic design and retrofit applications, this paper presents the results of a study comparing the properties of large diameter shape memory alloys to those of small wire specimens under cyclic loadings and loading rates typical of a seismic event. The results of a small-scale shake table test are then presented as a proof-of-concept study of a SMA cross-bracing system. These results are verified through analytical nonlinear time history analysis. Finally, a three-story steel frame implementing either a traditional steel buckling-allowed bracing system or a SMA bracing system is analyzed analytically and the maximum interstory drifts and residual drifts are compared to show the advantage of SMA bracing systems in seismic vibration control as compared to traditional steel bracing systems.

Material Testing of Wires and Bars

The behavior of NiTi shape memory alloys, particularly with respect to loading rates and loading levels typically caused by an earthquake, needs to be understood before implementing them into seismic vibration control applications in building structures. Since using larger diameter sections may be more economically convenient and easier to implement in SMA-based systems than NiTi wires, it is important to compare the behavior of larger diameter sections to wire specimens in order to determine how the size of the SMA specimen may affect the behavior. In order to evaluate the performance of the superelastic NiTi wires and bars, several of the mechanical properties are studied, including the residual strain (ε_R), the forward and reverse transformation stress (σ_L and σ_{UL}), the initial elastic modulus (E_i), and the equivalent viscous damping associated with a given cycle (ξ_{eq}). The residual strain provides a measure of the recentering capability of the SMA and refers to the strain at zero stress at the end of a strain cycle. The forward transformation stress is the stress at which the martensitic phase transformation initiates. The unloading plateau stress (or reverse transformation stress) is an estimate of the inflection point along the unloading curve corresponding to the reverse transformation from detwinned martensite back to the original austenite structure. The initial elastic modulus refers to the slope of the stress-strain curve prior to reaching the forward transformation stress. Typical earthquake engineering applications use equivalent viscous damping to measure the energy dissipation provided by a system where the equivalent viscous damping refers to the energy dissipated per cycle divided by the product of 4π and the strain energy for a complete cycle.

Small Wire Material Test Results. A number of 0.254 mm (0.01 in.) diameter superelastic NiTi wires were tested to determine the cyclic properties of small diameter wires. All of the specimens were straight annealed and had a black oxide surface. The specimens used for testing were all cut from the same 6.1 m (20 ft) length of wire with no additional annealing or processing being done to the material before testing. A tensile loading protocol simulating strain levels and strain rates that are experienced by structural members during an earthquake was developed consisting of strain cycles of 0.5%, 1.0–5.0% by increments of 1%, six cycles to 6%, and four cycles to 7% strain. Tests were run both quasi-statically (0.025 Hz) and dynamically (0.5–2.0 Hz) in order to capture any loading rate effects on those properties mentioned previously. All testing was done using a tabletop testing apparatus with an electromagnetic actuator. The loading protocol was implemented in displacement control with the strain levels being calculated based on the specimen gage length of ~38.1 mm (1.5 in.). All tests were run on previously untested specimen to simulate a newly installed seismic vibration control device with strains being measured based on the cross-head displacement and loads being measured with a 48.9 N (11 lbf) load cell.

The stress-strain results for the 0.025 Hz quasi-static and 1.0 Hz dynamic tests can be seen in Fig. 1. The plots all show the typical flag-shaped hysteresis associated with tensile cycling of superelastic NiTi SMAs. The results show a degradation of the unloading plateau with increased cycling rate and a slight increase in the residual strain at the higher loading rates. The quasi-static plot appears shifted to the right, suggesting possible slack in the wire at the onset of testing or a small amount of initial slipping during the first loading cycle. This suggests that the residual strain for the quasi-static test presented may be higher than their true values since strains were measured based on crosshead displacement. Even with the shifted curve, the residual strain remained below 1% when cycled to a maximum strain of 7% while the residual strains for the 1.0 Hz test was measured at 1.05% for the first 6% maximum strain cycle. At all loading rates, a slight degradation of the loading plateau stress occurred with increased cycling. This can be attributed to the formation of localized slip, which tends to assist the forward transformation. The loss of a clear unloading plateau with increased cycling rate can be attributed to a self-heating of the wire specimen due to the thermoelastic phase transformation. The increased temperature results in an increase and distortion of the unloading plateau during cycling. Cycling at higher rates does not allow time for produced heat from the exothermic/endothermic phase transformation to dissipate resulting in a more pronounced effect at higher strain rates. As a result of the increased unloading plateau and smaller increase in the loading plateau, the hysteretic area at higher strain rates

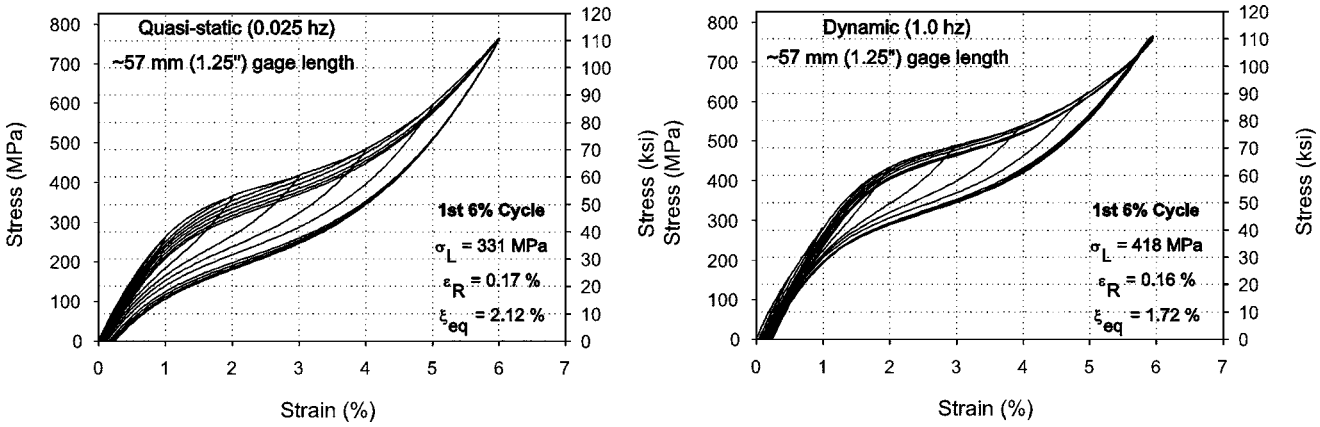

Fig. 2 Stress-strain curves for 12.7 mm (0.5 in.) diameter NiTi shape memory alloys tested at (*a*) 0.025 Hz and (*b*) 1.0 Hz loading rates [13]

decreases leading to a decrease in the equivalent viscous damping values with increased cycling from ~4.5% to ~4.1% for the first 6% strain cycle when tested quasi-statically and dynamically at 1.0 Hz, respectively.

Large Diameter Bar Material Test Results. A number of 12.7 mm (0.5 in.) diameter specimens were tested to determine the cyclic properties of larger NiTi superelastic shape memory alloy bars in order to see how bar size might influence the mechanical behavior of SMAs. These bars were tested in conjunction with those presented in DesRoches et al. [13]. All of the specimens were near equiatomic, cold drawn, and 30% cold worked prior to annealing. A similar tensile loading protocol to that used with the wire specimens presented above was implemented with the removal of the last two 6% strain cycles and the 7% strain cycles. A hydraulic testing apparatus fitted with hydraulic wedge grips was used to perform the tests at both a quasi-static loading rate of 0.025 Hz and a dynamic loading rate of 1.0 Hz. The loading protocol was implemented in strain control based on the feedback from a 25.4 mm (1.0 in.) gage length extensometer with the loads being measured by the internal load cell of the actuator. As with the small wire tests, all testing was conducted on previously untested specimens with gage lengths of 57 mm (2.25 in.).

Figure 2 provides the stress-strain curves for the cyclic tensile test performed on two of the 12.7 mm (0.5 in.) diameter NiTi specimens. As with the small wire specimens, both the quasi-static and dynamic specimens show good superelastic properties with the formation of a clear flag-shaped hysteresis and only small amounts of residual strain. The loading plateau stress has an increase of ~87 MPa (~12.6 ksi) with the increase in loading rate for the first 6% strain cycle. A similar increase can be seen in the unloading plateau stress, which, as was previously mentioned, can be attributed to a self-heating of the specimen during dynamic loading. The total residual strain for both large bar specimens remained small, suggesting that large diameter bars can still be used in recentering applications. The residual strain for the first 6% cycle did not change significantly between the quasi-static test and the dynamic test remaining at ~0.17%. Overall, the larger diameter specimens had smaller hysteresis loops as compared to the small wire specimens, resulting in significantly smaller damping capacity compared to the wires. The equivalent viscous damping values suggest that larger diameter superelastic NiTi SMAs cannot provide usable damping quantities. The test results also show a decrease of ~0.4% in the equivalent viscous damping when cycled dynamically as compared to the quasi-static test results.

Cyclic Properties of Wires and Bars. The plots in Fig. 3 provide the residual strain and equivalent viscous damping values with respect to the maximum cyclic strain for the 0.254 mm (0.01 in.) diameter NiTi wires and the 12.7 mm (0.5 in.) diameter bars tested quasi-statically and dynamically at 1.0 Hz. The variation in the residual strain with respect to maximum cyclic strain and loading rate can be seen in Fig. 3(*a*). For all specimens and

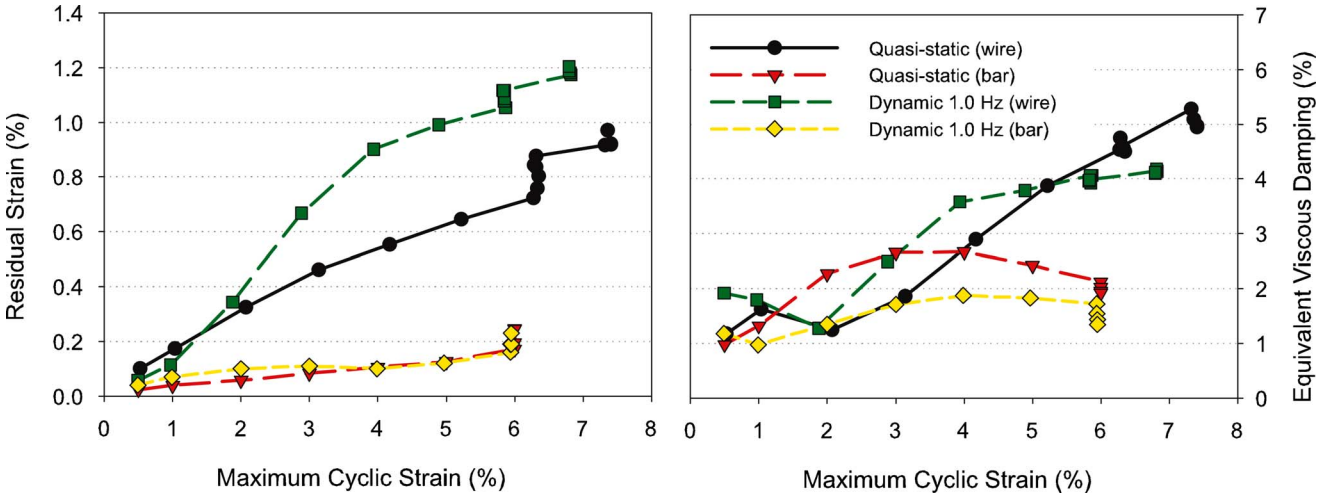

Fig. 3 Cyclic properties comparison of NiTi shape memory alloys: (*a*) residual strain and (*b*) equivalent viscous damping

loading rates, the residual strain increased with increased cycling due to the formation and accumulation of permanent localized slip, which inhibits the reverse transformation and the shape recovery process. The wire specimens had larger residual strain values for a given maximum cyclic strain cycle as compared to the larger diameter bar specimens. For the quasi-static loading rates, the maximum residual strains for the fourth 6% strain cycle were ~0.84% and ~0.25% for the wire specimen and the bar specimen, respectively. Increasing the loading rate to 1.0 Hz led to residual strains of ~1.12% and ~0.23% after the fourth 6% strain cycle for the wire specimen and bar specimen, respectively. The results show a clear influence of bar size on the accumulation of residual strain with larger diameter specimens providing lower residual strain values and, thus, better recentering capabilities. Loading rate appears to have less of an effect on the residual strain values, particularly for the larger diameter specimens. This result suggests that NiTi SMAs may be ideal as recentering devices in seismic vibration control applications.

Figure 3(*b*) provides the variation in the equivalent viscous damping values with respect to maximum cyclic strain and strain rate for the 0.254 mm (0.01 in.) diameter superelastic NiTi wires and 12.7 mm (0.5 in.) diameter superelastic bars. The results clearly show that the wire specimens provide much higher damping capacity as compared to the larger diameter bar specimens. During quasi-static cycling, the maximum equivalent viscous damping values decreased from ~5.27% for the wire specimen to 2.67% for the bar specimen. A similar decreased damping capacity was found for the specimens tested dynamically, suggesting a clear influence of bar size on the damping capacity of superelastic SMAs. The maximum equivalent viscous damping values also decreased with increased strain rate for both size specimens. The decrease was ~1% equivalent viscous damping for both size specimens when comparing the quasi-static test results and the dynamic 1.0 Hz test results. The reduced damping with increased strain rate can be associated with an increase and distortion of the unloading plateau stress and the decrease in the loading plateau stress with increased strain rate resulting in a decrease in the hysteretic area. It is important to note that the equivalent viscous damping values tend to be too low to be used in a purely damping device. Although combined with the low residual strain values, superelastic NiTi SMAs provide a unique combination of damping and recentering capabilities that are optimal for structural vibration control.

Small Shake Table Proof-of-Concept Test

In order to initially establish the ability of superelastic SMAs to reduce the structural response and control seismic vibration of a building under earthquake loadings, a reduced scale proof-of-concept model was developed that could be tested on a small 457 mm (18 in.) by 457 mm (18 in.) shake table. The model consisted of three stories with constant story heights of 295 mm (11.6 in.) and a single bay of width 254 mm (10 in.). The floors were made out of two sheets of Plexiglas to create a rigid floor system, and the columns used were circular, hollow brass rods. A weight of ~2.93 kg (~6.5 lb) was placed on each floor to ensure that the SMA braces would undergo the phase transformation during shaking. The structure was designed so that the wire (tension-only) cross braces are installed in the bays parallel to the direction of motion. The braced structure can be seen in Fig. 4. The same 0.254 mm (0.01 in.) diameter SMA wires tested previously were used as the bracing system during this study. Both the unbraced and braced structures were tested on the shake table under the LA 21 SAC ground motion [14] scaled to a PGA of 1.0 g. The acceleration results from the accelerometers placed on the second and third floors showed an increase in maximum acceleration experienced when the SMA braces were installed as a result of the higher stiffness associated with the braced structure as compared to the unbraced structure. Although the accelerations were higher

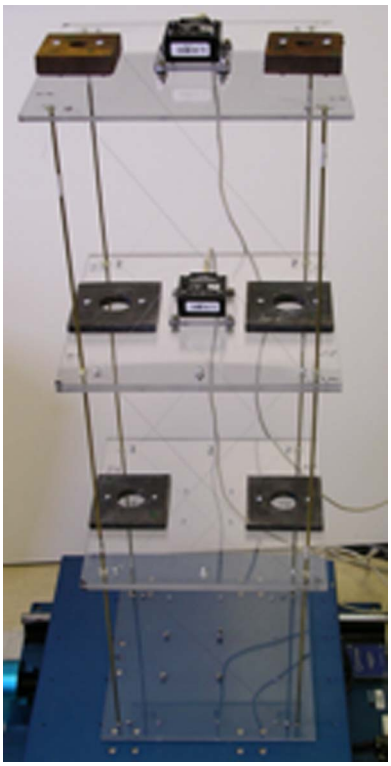

Fig. 4 Proof-of-concept shake table model with 0.254 mm (0.01 in.) diameter SMA braces

for the braced structure, the damping and recentering capability of the wires tended to decrease the response at a faster rate than the unbraced structure.

Since only limited results could be obtained from the small shake table study, an analytical model of the proof-of-concept structure was developed in OpenSEES [15]. The mechanical properties of the brass columns were obtained through laboratory testing, and the properties of the SMA wires were obtained from the cyclic tensile tests of the 0.254 mm (0.01 in.) diameter wires presented previously. Detailed information of the SMA model can be found in the following sections of this paper. The accelerations obtained from the accelerometer on the shake table were used as the input ground motion for the analysis. The resulting displacement time history for the roof can be seen in Fig. 5. The

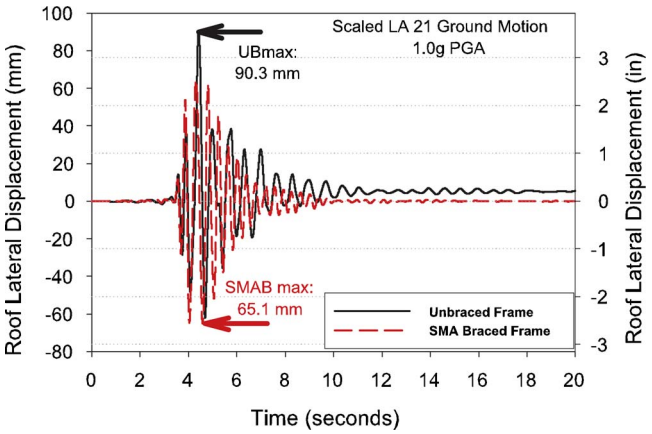

Fig. 5 Analytical displacement time history of the roof for the proof-of-concept model undergoing the LA21 ground motion scaled to 1.0 PGA

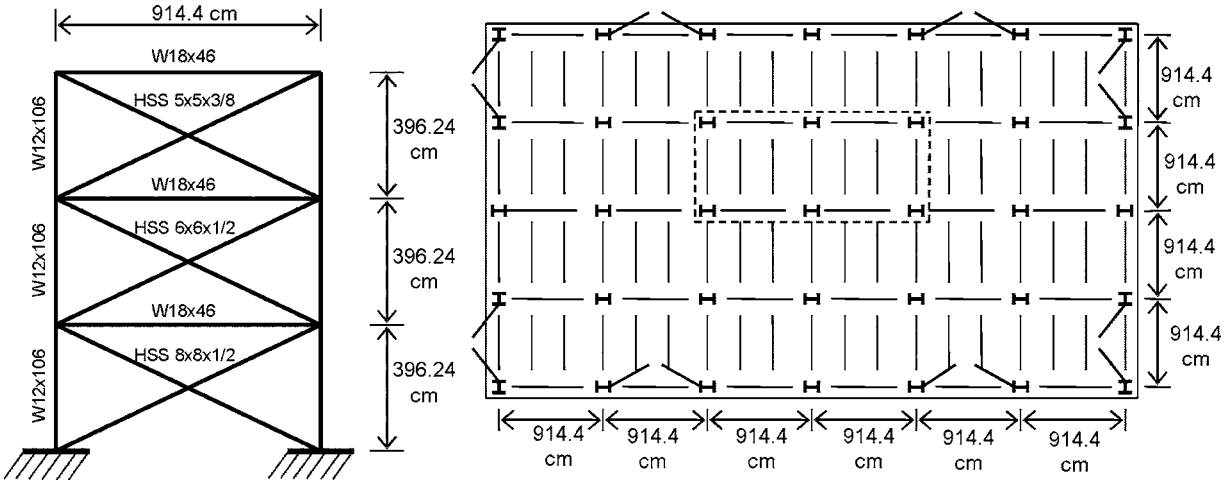

Fig. 6 Elevation and plan view of the three-story frame

results show a significant decrease in the maximum roof displacement from 90.3 mm (3.56 in.) for the unbraced structure to 65.1 mm (2.56 in.) for the SMA braced structure. The residual drift of the roof was improved with the use of SMA braces from 5.0 mm (0.2 in.) to 0.11 mm (0.004 in.). The proof-of-concept results suggest that a SMA bracing system can be used for seismic vibration control in structures, although a suitable structural system must be determined and comparisons must be made with current earthquake mitigation techniques to determine whether SMA systems are a suitable option for supplemental energy dissipation and recentering.

Analytical Study of a Concentrically Braced Steel Frame

In recent years, studies have been conducted by Sabelli [16] and Sabelli et al. [17] on the seismic response of concentrically braced steel frames. The research was undertaken to address the damage caused by recent earthquakes to concentrically braced steel frames by better determining the seismic demand on steel braced structures and improving design techniques. Concentrically braced steel frames are important in seismic design because of the susceptibility of steel moment resisting frames to large lateral displacements. Sabelli [16] and Sabelli et al. [17] found that concentric steel bracing systems performed well, particularly with the use of buckling restrained braces, although few design approaches using buckling restrained braces exist. The use of conventional steel braces also can result in yielding and permanent damage to the bracing system requiring extensive repair to the structure after an earthquake. The material studies and proof-of-concept model presented above suggests that the use of SMAs in a concentric bracing system can address these problems. The recentering capability and added damping associated with the flag-shaped hysteresis of large diameter superelastic SMAs provide a unique way to reduce the seismic response of steel braced frames.

In order to compare the seismic response of a conventional steel braced frame, in which the steel braces are allowed to buckle, to a superelastic SMA bracing system, the three-story cross-braced frame presented by Sabelli [16] is considered. Only a single braced bay is studied based on the symmetry of the structure. The geometric properties and member sizes are given in Fig. 6 for the conventional steel braced structure. The second structure implementing the innovative SMA braces is shown in Fig. 7 where the beam and column members are sized the same as the conventional steel braced structure. The SMA braces consist of a rigid segment connected to an SMA member in order to ensure that the deformation occurs in the SMA segment of the brace. This is a conceptual representation of an SMA bracing system implementing large diameter bars in which the bracing system itself is configured so that the majority of the deformation occurs in the less stiff SMA specimen with the remainder of the bracing system made of a significantly stiffer member so as to only undergo minimal deformation and no buckling. It is acknowledged that the actual non-SMA segment may undergo some deformation in an actual bracing device, resulting in somewhat higher displacements; but for the purpose of this conceptual study, a rigid segment is assumed. By configuring the SMA brace in this manner, the initial stiffness of the bracing system can be adjusted with respect to the length of the SMA segment and cross-sectional area of SMA material used. The properties of the SMA segment are given in Table 1. In order to compare the effectiveness of the SMA braces to the conventional steel braces, they are designed to provide the same axial stiffness and yield strength as the conventional steel braces, resulting in both structures having the same initial natural period. The performance of the two braced frames is measured based on maximum interstory drift and the residual drift associated with the top floor. A suite of ten LA ground motions with a 10% probability of

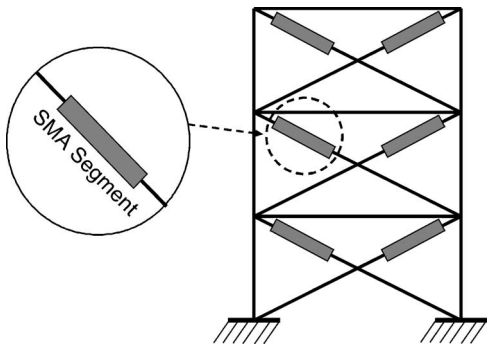

Fig. 7 Detail of the innovative SMA braces in the three-story frame

Table 1 Geometric characteristics of SMA segments

	SMAs braces for three-story frame	
Story	Length (mm (in.))	Area (mm^2 ($in.^2$))
1	829.84 (32.67)	5259.46 (8.15)
2	829.84 (32.67)	3794.60 (5.88)
3	829.84 (32.67)	2407.66 (3.73)

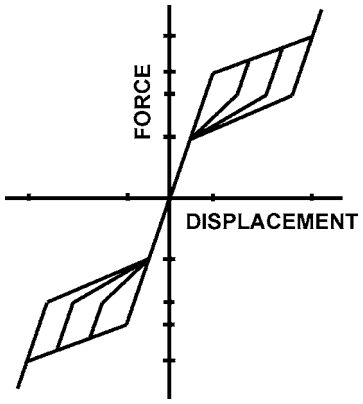

Fig. 8 Force-displacement relationship for the SMA braces

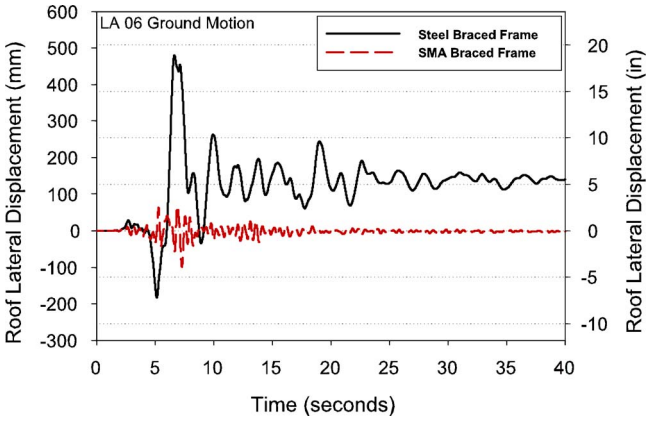

Fig. 9 Displacement time history of the roof experienced in the three-story frame excited by the LA06 record

exceedance in 50 years developed for the SAC building study are used in the nonlinear time history analysis to evaluate the structures [14].

The nonlinear dynamic time history analyses are carried out using the OpenSEES [15] platform. For the simulation, the beam and column elements are modeled using nonlinear elements with fiber sections. A uniaxial steel material model is applied to these elements. Fixed connections are assumed throughout the structure except at the roof level where the beam-column connection is modeled as pinned. The braces are pinned at either end in order to ensure that they only carry axial load. P-Δ effects are taken into account, and a 5% Rayleigh damping is specified based on typical values adopted for steel structures [16,17].

The conventional steel braces are modeled with a modified version of the hysteretic model that takes into account buckling under compression. The material properties used for the steel braces are those specified in Sabelli [16]. The superelastic SMAs are modeled using a modified uniaxial constitutive model proposed by Auricchio and Sacco [18]. The formulation, developed in the small deformation region, assumes that the stress-strain relationship can be represented by straight segments whose form is determined by the extent of the transformation experienced. Further assumptions that no strength degradation occurs during cycling [19] and that the austenite and martensite branches have the same modulus of elasticity [20] are made. The model for the SMA braces is shown in Fig. 8. Details in regard to the continuous model and its integration techniques are given in the work by Fugazza [21]. The properties of the SMA braces are based on the dynamic experimental tests on the 12.7 mm (0.5 in.) diameter superelastic NiTi specimens presented previously. It is assumed that the large cross section allows the SMA segment to sustain both tension and compression. Buckling of the SMA bars is prevented by encasing the SMA bars in a grouted tube in which the SMA bars are unbonded to allow for shape recovery.

The results of the analytical analysis of the three-story braced frame for the La06 ground motion are shown in Figs. 9 and 10 for the conventional steel braced and SMA braced buildings. Figure 9 provides the lateral displacement time history of the upper left node of the structure. The maximum roof displacement is decreased significantly with the use of the SMA bracing system as compared to the conventional buckling-allowed bracing system. The maximum lateral roof displacements are ~480 mm (~18.9 in.) for the steel braced frame as compared to ~99 mm (3.9 in.) for the SMA braced frame resulting in a 79% reduction in the maximum roof displacement. In general, the large roof displacement of the steel braced frame suggests possible collapse due to instability associated with P-Δ effects, but collapse of the structure is not considered as part of this analysis. The force-displacement curves for the bottom brace of both structures undergoing the LA06 ground motion are shown in Fig. 10. The steel brace underwent larger deformations compared to the SMA brace. This can be attributed to the steel braces experiencing early buckling, resulting in a decrease in stiffness with respect to the SMA braces and a significant accumulation of residual strain. The SMA braces reached the forward transformation stress in negative deformation, but the recentering capability of the SMA resulted in no permanent residual deformation. The results suggest that the braces in a SMA braced frame would not have to be replaced given the minimal deformations (~24 mm (~0.95 in.)) experienced as opposed to conventional steel braces which have yielded and permanently deformed. The ability of the SMA bracing system to maintain its initial stiffness, accumulate no residual strain, and sustain both tensile and compressive loadings results in a reduction in the response of the frame.

Given the performance of the shape memory alloy bracing system, a third structure was analyzed that implemented one-half the cross-sectional area and one-half the length of the initial SMA bracing system shown in Table 1. The reduced SMA braced structure has the same natural period as the other two structures because of the reduction of both the cross-sectional area and the length, but the braces undergo the phase transformation at one-half the force of the original SMA structure. Plots of the maximum interstory drift and residual drift of the top floor with respect to the ten ground motions are shown in Fig. 11. The results provide evidence that superelastic SMA braces reduce the maximum interstory drift for concentrically braced frames compared to buckling-allowed steel bracing systems. In all cases, the SMA braced structure and reduced SMA braced structure have a maximum interstory drift of $<1.1\%$ and $<1.25\%$, respectively, where the smallest maximum interstory drift for the conventional steel braced frame is ~1.3%. On average, the original SMA braced frame sustained maximum interstory drifts of 2.78% (reduction of 76%) less than those experienced by the conventional steel braced frame. These results can be attributed to the recentering capability of the superelastic SMAs, resulting in less accumulation of residual strain in the bracing members and the SMA bracing system maintaining its initial stiffness for low strain cycles. Comparing the original SMA braces to the reduced SMA braces, the maximum interstory drift only increased by ~0.14% as a result of the decreased SMA area. This result suggests that smaller amounts of SMA material can be used in bracing systems, which would help to reduce the cost of such a system.

The top floor residual drift results provide further evidence of the effectiveness of the innovative bracing systems. The maximum residual drift sustained by the steel braced, SMA braced, and reduced SMA braced structures are 1.19%, 0.013%, and 0.031%, respectively. For all of the ground motions, the SMA braced and reduced SMA braced structure underwent only small residual drifts as compared to the conventional steel braced structure as a

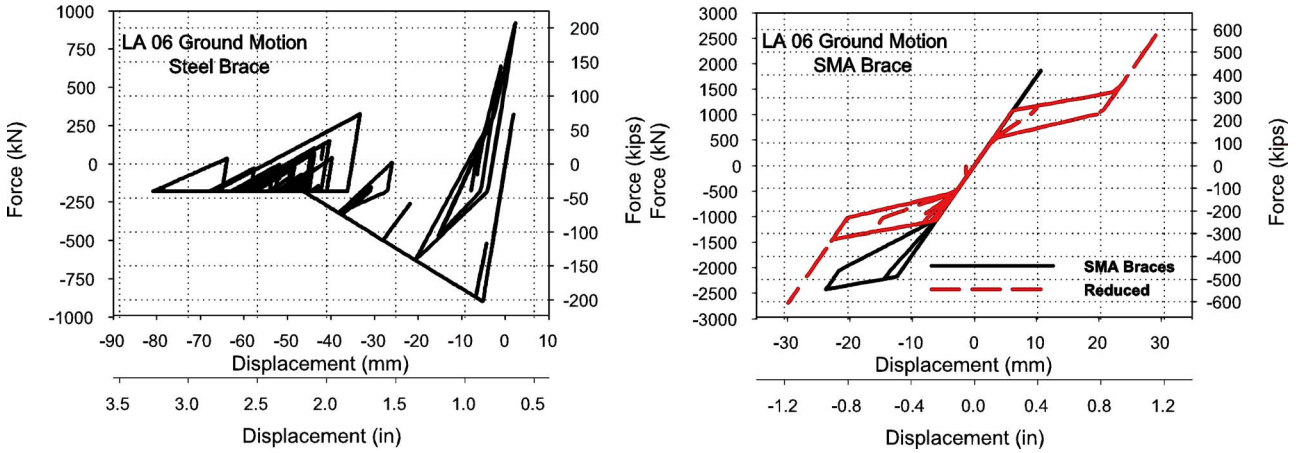

Fig. 10 Force-displacement relationship experienced by one of the bottom braces excited by the LA06 record: (*a*) steel brace and (*b*) SMA brace

result of the recentering capability. The steel braces underwent permanent yielding and buckling, reducing the effectiveness of the steel braces when a number of larger displacement cycles occur. Given the maximum roof displacements of some of the steel braced frames, it is also suggested that larger residual strains could be associated with the steel braced structures if collapse or partial collapse is considered. The residual drifts of the reduced SMA structure compared favorably to those of the original SMA braced structure with residual drift remaining considerably low compared to the steel braced structure. This result further suggests that a reduced area of SMA can be used in seismic applications. Overall, the superelastic SMA bracing system proved to reduce the structural vibration more effectively than the conventional steel braces.

Conclusion

This study considered the use of superelastic shape memory alloys for seismic vibration control of typical structures. The ability of superelastic SMAs to undergo large deformation while returning to their original undeformed shape by undergoing a unique displacive (diffusionless) martensitic phase transformation provides a means to control structural vibration through a combination of recentering capability and hysteretic damping. Both small diameter superelastic NiTi wire and larger diameter superelastic NiTi bars showed good superelastic behavior under uniaxial tensile cyclic loads equivalent to an earthquake. Under both quasi-static and dynamic loadings, both size specimens produced the flag-shaped hysteresis associated with the superelastic effect with only a small distortion to the unloading plateau at larger strain levels. In general, the residual strains for the wire specimens after several 6% strain cycles were between 70% and 80% higher than those found for the larger diameter bar specimens. However, in all cases, the residual strain remained below 1.2%, suggesting that both small wires and larger diameter bars, which may be more economical for structural vibration control, can provide recentering capabilities up to strain levels associated with seismic events. The damping capacity was found to be higher for the wire specimens by ~2–3% equivalent viscous damping as compared to the bar specimens; however, the low equivalent viscous damping values suggest that superelastic SMAs should not be used as purely damping devices. The material test results suggest that SMA wire or bars can provide recentering capability and some added damping capacity to a structure when implemented as vibration control or recentering devices in structures.

The results of the materials study were used to calibrate a three-story small scale proof-of-concept model containing superelastic SMA braces that was run on a small-scale shaking table. The results showed an increase in the floor accelerations with the implementation of SMA braces as opposed to the unbraced structure. Although the accelerations increased, the rate at which the structural vibrations damped out was faster when the SMA braces were used. Furthermore, an analytical model of a three-story steel

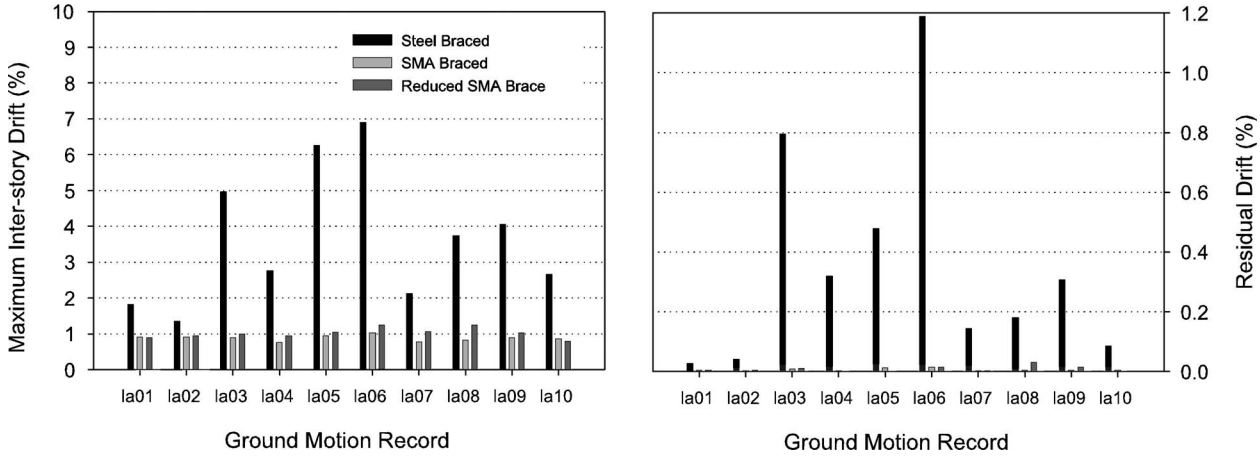

Fig. 11 (*a*) Maximum interstory drift and (*b*) residual drift of the top floor exhibited by the three-story steel braced frame with either conventional steel braces, innovative SMA braces, or innovative SMA braces with a reduced cross-sectional area

frame with either a conventional steel buckling-allowed cross-bracing system or a superelastic SMA cross-bracing system was developed. The dynamic performance under seismic inputs of the two bracing configurations is evaluated. The results showed significant decreases in the maximum interdrift values with the use of SMA braces and almost no residual displacements due to the re-centering capability of the SMA material and the ability of the SMA braces to resist buckling. The conventional steel braces underwent yielding and buckling, resulting in permanent story drifts and less effective seismic vibration control. The results suggest that a comparison of SMA braces that can sustain only tension loadings with conventional steel braces and a comparison of buckling-restrained steel braces to SMA tension-compression braces may provide further insight into the viability of using SMA braces, particularly in terms of reducing residual drifts. More accurate models of the SMA bracing system behavior can then be studied as actual systems implementing large diameter sections are constructed and tested.

The goal of this study was to illustrate the use of superelastic SMAs in seismic response control of civil engineering structures through added recentering capability. The results show that the larger diameter bars perform as well as wire specimens that are currently being used in non-civil-engineering applications. More importantly, the unique properties of SMAs appear to provide a means of reducing vibration response of a structure during seismic events, although further research is needed in order to determine methods to increase the damping capacity of SMAs and reduce the degradation of some of the superelastic properties under high strain rates.

Acknowledgment

This study has been supported primarily by the CAREER Program of the National Science Foundation under Grant No. 0093868. Davide Fugazza would like to acknowledge the Italian National Seismic Survey (Rome, Italy) for providing the Ph.D. Scholarship as well as the University of Pavia (Pavia, Italy) for the financial support.

Nomenclature

E_i = initial modulus of elasticity
SMA = shape memory alloy
ε_R = residual strain
σ_L = loading plateau stress
σ_{UL} = unloading plateau stress
ξ_{eq} = equivalent viscous damping ratio

References

[1] Eguchi, R. T., Goltz, J. D., Taylor, C. E., Chang, S. E., Flores, P. J., Johnson, L. A., Seligson, H. A., and Blais, N. C., 1998, "Direct Economic Losses in the Northridge Earthquake: A Three-Year Post-Event Perspective," Earthquake Spectra, **14**(2), pp. 245–264.

[2] Piedboeuf, M. C., Gauvin, R., and Thomas, M., 1998, "Damping Behavior of Shape Memory Alloys: Strain Amplitude, Frequency and Temperature Effects," J. Sound Vib., **214**(5), pp. 885–901.

[3] Wolons, D., Gandhi, F., and Malovrh, B., 1998, "Experimental Investigation of the Pseudoelastic Hysteresis Damping Characteristics of Shape Memory Alloy Wires," J. Intell. Mater. Syst. Struct., **9**(2), pp. 116–126.

[4] Hodgson, D. E., 2002, "Damping Applications of Shape-Memory Alloys," Mater. Sci. Forum, **394–395**, pp. 69–74.

[5] Dolce, M., and Cardone, D., 2001, "Mechanical Behavior of Shape Memory Alloys for Seismic Applications: Part 2—Austenite Wires Subjected to Tension," Int. J. Mech. Sci., **43**(11), pp. 2657–2676.

[6] Dolce, M., Cardone, D., Marnetto, R., Mucciarelli, M., Nigro, D., Ponzo, F. C., Santarsiero, G., 2004, "Experimental Static and Dynamic Response of a Real R/C Frame Upgraded With SMA Re-Centering and Dissipating Braces," *Proceeding of 13th World Conference on Earthquake Engineering*, Vancouver, Mira Digital Publishing, St. Louis, MO, Paper No. 2878.

[7] Cardone, D., Coelho, E., Dolce, M., and Ponzo, F. C., 2004, "Experimental Behaviour of R/C Frames Retrofitted With Dissipating and Re-centering Braces," J. Earthquake Eng., **8**(3), pp. 361–396.

[8] Dolce, M., Cardone, D., Ponzo, F. C., and Valente, C., 2005, "Shaking Table Tests on Reinforced Concrete Frames Without and With Passive Control Systems," Earthquake Eng. Struct. Dyn., **34**(14), pp. 1687–1717.

[9] Baratta, A., and Corbi, O., 2002, "On the Dynamic Behaviour of Elastic-Plastic Structures Equipped With Pseudoelastic SMA Reinforcements," Comput. Mater. Sci., **25**, pp. 1–13.

[10] Clark, P. W., Aiken, I. D., Kelly, J. M., Higashino, M., and Krumme, R. C., 1995, "Experimental and Analytical Studies of Shape Memory Alloy Dampers for Structural Control," Proc. SPIE, **2445**, pp. 241–251.

[11] Sweeney, S. C., and Hayes, J. R., Jr., 1995, "Shape Memory Alloy Dampers for Seismic Rehabilitation of Existing Buildings," *Proceedings of 27th Joint Meeting on Wind and Seismic Effects*, Tsukuba, Japan, Public Works Research Institute, Tsukuba, Japan, pp. 317–332.

[12] Inaudi, J., and Kelly, J., 1994, "Experiments on Tuned Mass Dampers Using Viscoelastic, Frictional and Shape-Memory Alloy Materials," *First World Conference on Structural Control*, Los Angeles, pp. 127–136.

[13] DesRoches, R., McCormick, J., and Delemont, M., 2004, "Cyclic Properties of Superelastic Shape Memory Alloy Wires and Bars," Adv. Environ. Res., **130**(1), pp. 38–46.

[14] Somerville, P., Smith, N., Punyamurthula, S., and Sun, J., 1997, "Development of Ground Motion Time Histories for Phase 2," Report No. SAC-BD.97-04, SAC Joint Venture, Richmond, CA.

[15] McKenna, F., and Fenves, G., 2003, *The OpenSees Command Language Manual*, Pacific Earthquake Engineering Center, Univ. of Calif., Berkeley, http://opensees.berkeley.edu

[16] Sabelli, R., 2001, "Research on Improving the Design and Analysis of Earthquake-Resistant Steel-Braced Frames," Professional Fellowship Report No. PF2000-9, NEHRP, Washington, DC.

[17] Sabelli, R., Mahin, S., and Chang, C., 2003, "Seismic Demands on Steel Braced Frame Buildings With Buckling-Restrained Braces," Eng. Struct., **25**, pp. 655–666.

[18] Auricchio, F., and Sacco, E., 1997, "A One-Dimensional Model for Superelastic Shape-Memory Alloys With Different Properties Between Martensite and Austenite," Int. J. Non-Linear Mech., **32**, pp. 1101–1114.

[19] McCormick, J., and DesRoches, R., 2003, "Seismic Response Reduction Using Smart Bracing Elements," *Extreme Loadings Conference: Response of Structures to Extreme Loadings*, Toronto.

[20] Andrawes, B., McCormick, J., and DesRoches, R., 2004, "Effect of Cyclic Modeling Parameters on the Behavior of Shape Memory Alloys for Seismic Applications," Proc. SPIE, **5390**, pp. 324–334.

[21] Fugazza, D., 2003, "Shape-Memory Alloy Devices for Earthquake Engineering: Mechanical Properties, Constitutive Modeling and Numerical Simulations," Masters' thesis, European School for Advanced Studies in Reduction of Seismic Risk, Pavia, Italy.